DOI 10.1007/s11595-015-1129-2

Synthesis of Low-cost $LiFePO_4$ from Li_2CO_3 by a Novel Hydrothermal Method and Investigation on the Reaction Mechanism

LI Xiangfeng, HU Yunlong, LIU Fang, ZHANG Zhao*
(College of Chemical Engineering, Sichuan University, Chengdu 610065, China)

Abstract: Phspho-olivine $LiFePO_4$ was synthesized from the relatively insoluble lithium source Li_2CO_3, proper iron and phosphorus sources (*n*(Li):*n*(Fe):n(P)=1:1:1) by a novel hydrothermal method. Afterwards, the optimal sample was mixed with glucose and two-step calcinated (500 ℃ and 750 ℃) under high-purity N_2 to obtain the $LiFePO_4$/C composite. The resultant samples were characterized by X-ray diffraction (XRD), atomic absorption spectrometry (AAS), scanning electron microscops (SEM), transmission electron microscopy (TEM), energy dispersive spectrometry (EDS), elementary analysis (EA) and electrochemical tests. The results show that the optimal reaction condition is to set the reactant concentration at 0.5 mol · L^{-1}, the reaction temperature at 180 ℃ for 16 h duration. During the reaction course, an intermediate product NH_4FePO_4•H_2O was first synthesized, and then it reacted with Li^+ to form $LiFePO_4$. The optimized $LiFePO_4$ sample with an average particle size (300 to 500 nm) and regular morphology exhibits a relatively high discharge capacity of 84.95 mAh · g^{-1} at the first charge-discharge cycle (0.1C, 1C=170 mA · g^{-1}). Moreover, the prepared $LiFePO_4$/C composite shows a high discharge capacity of 154.3 mAh · g^{-1} at 0.1C and 128.2 mAh · g^{-1} even at 5C. Besides it has good reversibility and stability in CV test.

Key words: Li-ion battery; $LiFePO_4$; hydrothermal method; Li_2CO_3; reaction mechanism

1 Introduction

In 1997, phspho-olivine $LiFePO_4$ was first introduced as a possible cathode for rechargeable Li-ion batteries by Padhi *et al*[1]. Due to its low cost, high theoretical capacity (170 mAh · g^{-1}), non-toxicity, and high stability, $LiFePO_4$ has become an attractive substitution for the currently used $LiCoO_2$ or $LiMn_2O_4$ cathodes[2]. However, the performance of $LiFePO_4$ is limited by its poor electronic conductivity (10^{-9} to 10^{-8} S · cm^{-1}), ionic conductivity (10^{-11} to 10^{-9} S · cm^{-1}) and low diffusivity (10^{-17} to 10^{-14} cm^2 · S^{-1})[3,4], which have become the main obstacles for its applications. The numerous approaches directed at overcoming these problems have been reported in the past decade. These include adopting various synthetic methods, systematic control of reaction parameters and material modification to enhance the performance of $LiFePO_4$[5,6]. Recent results show that small particle size and kinetically favorable morphology could shorten the diffusion path of ions in $LiFePO_4$[7,8], and the synthetic method has an important effect on the particle size and morphology[9]. Compared with solid-state, sol-gel and co-precipitation processes, hydrothermal method arouses particular interest due to its mild operating conditions, simple process and the potential for scale-up production of $LiFePO_4$[10-13]. Moreover, the hydrothermal method is also considerably convenient to promote the performances of the $LiFePO_4$ products by adjusting experimental parameters such as concentration, temperature, pressure and reaction duration, *etc*[14].

Although hydrothermal method has been particularly successful in offering high-performance $LiFePO_4$ in several researches, the waste of lithium source has not been solved effectively[15-18]. In order to obtain $LiFePO_4$ with pure phase, the excessive

(Received: Mar. 19, 2014; Accepted: Apr. 28, 2014)
LI Xiangfeng (李向锋): Ph D Candidate; E-mail: hkdlixiangfeng@163.com
*Corresponding author: ZHANG Zhao (张昭): Prof.; Ph D; E-mail: zzhang@scu.edu.cn
Funded by the National Natural Science Foundation of China (No. 51004074)

lithium source is usually required. For example, Brochu F *et al*[15] applied LiOH, $FeSO_4 \cdot 7H_2O$, H_3PO_4 as the starting materials (n(Li):n(Fe):n(P)=3:1:1), the excessive lithium source existed in the solution in the form of Li_2SO_4 instead of $LiFePO_4$. If the hydrothermal method is applied in scale-up production of $LiFePO_4$, the excessive lithium source should be recycled because the price of lithium salt is relatively high. But doing so will lead the technical process complicated and increase the cost of $LiFePO_4$. Recently, Recham N *et al*[19] reported that $LiFePO_4$ could be synthesized from LiH_2PO_4 and $FeSO_4 \cdot 7H_2O$ (molar ratio, 1:1) through hydrothermal method. However, the price of LiH_2PO_4 is relatively high and it is not common in industry.

In this study, a novel hydrothermal method was proposed to prepare low-cost and high-performance $LiFePO_4$. The insoluble Li_2CO_3 was used to replace the traditional soluble lithium source, $(NH_4)_2Fe(SO_4)_2 \cdot 6H_2O$ and $(NH_4)_2HPO_4$ were used as the ferrous and phosphoric sources, respectively (n(Li):n(Fe):n(P)=1:1:1). Although Li_2CO_3 is usually used as lithium source in the solid-state method for preparing $LiFePO_4$[20,21], the reports about it being applied to the hydrothermal method have rarely been referred to. The novel hydrothermal method takes advantage of both the coating-precipitation process and the hydrothermal process[22-24]: on the one hand, the insoluble Li_2CO_3 is used as the core of the coating-precipitation precursor to fully utilize the lithium source; on the other hand, the hydrothermal process is convenient to obtain the high-performance $LiFePO_4$ products by adjusting the reaction conditions. At the same time, the mechanism of converting the coating-precipitation precursor with core-shell structure to the $LiFePO_4$ product was also investigated. In addition, the $LiFePO_4$/C composite obtained from two-step calcinations (500 ℃ and 750 ℃) of the mixture of the optimal $LiFePO_4$ sample and glucose under high-purity N_2[14,25] exhibits excellent electrochemical performance with respect to discharge capacity, rate capability and cycling performance.

2 Experimental

$LiFePO_4$ samples were prepared by the novel hydrothermal method using a 100 mL stainless-steel reactor inside a PTFE vessel. The starting materials were Li_2CO_3 (A.R.), $(NH_4)_2Fe(SO_4)_2 \cdot 6H_2O$ (A.R.), $(NH_4)_2HPO_4$ (A.R.) in stoichiometric ratio (1:2:2). $(NH_4)_2Fe(SO_4)_2 \cdot 6H_2O$ and $(NH_4)_2HPO_4$ were dissolved in deionized water separately. A small amount of ascorbic acid was also added to the $(NH_4)_2Fe(SO_4)_2 \cdot 6H_2O$ solution, which could minimize the oxidation of Fe^{2+} to Fe^{3+}. Then the two solutions were mixed with a fixed sequence under magnetic stirring in a beaker containing Li_2CO_3 powder, and the beaker was heated in a boiling water bath. Meanwhile, the pH value of the solution was adjusted to a set value (pH=7) using ammonia solution. The concentration of the reaction solution was controlled to be 0.25, 0.50, 1.00 mol $\cdot L^{-1}$ (according to Li^+), respectively. The resulting grayish-green slurry (the total volume 80 mL) was transferred into the autoclave, sealed and heated in an oven. The oven was set at a certain temperature and duration. After the reaction, the products were cooled to room temperature, filtered and washed with deionized water and absolute ethanol, then dried in a vacuum oven at 120 ℃ for 2 h to obtain the grayish colored $LiFePO_4$ samples.

In addition, the optimal $LiFePO_4$ sample was mixed with glucose at a weight ratio of 9:1 and then the mixture was blended in a powder mixer for 10 min to get well mixed powders. The mixture was calcined by two-step in a tube furnace at 500 ℃ for 1h and 750 ℃ for 4 h under a N_2 (99.99%) flow. After cooling, the $LiFePO_4$/C composite was obtained.

The phase identification of the samples was performed with an X-ray diffractometer (XRD, Philips X'pert Pro MPD) with a Cu Kα radiation (λ=1.54178 Å). The lattice parameters of the samples were calculated by the software of Jade 5.0. The morphology of the samples was characterized by a scanning electron microscope (SEM, Jeol JEM-5900LV). The chemical composition of the $LiFePO_4$ sample and the concentration of Li^+ in the reaction solution were determined by an atomic absorption spectrophotometer (AAS, SpectrAA 220FS). The core-shell structure of the coating-precipitation precursor was characterized by a transmission electron microscope (TEM, Tecnai G^2F20S-TWIN) and an energy dispersive spectrophotometer (EDS, X-Max 51-XMX0019). The weight percentages of carbon in the $LiFePO_4$/C composites were determined by an elemental analyzer (EA, Italy Euro EA 3000).

The electrochemical performances of the samples were investigated via CR2032 coin-type model cells assembled in an argon-filled glove box. Each cell was composed of a lithium anode and a $LiFePO_4$ or $LiFePO_4$/C cathode. The cathode was prepared

by blending the $LiFePO_4$ or $LiFePO_4$/C composite, acetylene black, and the binder (7.5wt% polyvinylidene fluoride in N-methy l-2-pyrrolidinone) at the weight ratio of 80:15:5; then, the mixture was rolled into a thin sheet with uniform thickness on the aluminum foil and cut to the fixed size to fit the CR2032 shell. The used electrolyte was 1 mol · L^{-1} $LiPF_6$ in a 1:1 mixture of ethylene carbonate (EC) and diethyl carbonate (DEC). Celegard 2700 membrane was used as the separator. The galvanostatic cycling tests were carried out on a battery test system (Newell, China) with a voltage cutoff of 4.3-2.5 V at room temperature. The cyclic voltammetry curves were recorded on the electrochemical workstation (CHI660C, China) in the voltage range of 2.5-4.3 V at a constant scanning rate of 0.1 mV · s^{-1}.

3 Results and discussion

3.1 Investigation of the optimal reaction condition

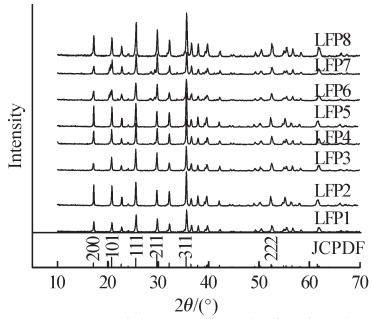

Fig.1 XRD patterns of the samples obtained under different reactant conditions

Table 1 Lattice parameters and yields of the $LiFePO_4$ and $LiFePO_4$/C samples

Sample	Latttice parameters			Cell volume /nm^3	Yield /%
	a/nm	b/nm	c/nm		
LFP1	0.5991	1.0336	0.4710	0.2917	96.32
LFP2	0.6011	1.0347	0.4707	0.2927	97.17
LFP3	0.5996	1.0337	0.4693	0.2909	97.31
LFP4	0.5990	1.0343	0.4697	0.2910	96.58
LFP5	0.5995	1.0340	0.4697	0.2912	97.22
LFP6	0.5996	1.0340	0.4698	0.2913	96.11
LFP7	0.5996	1.0333	0.4693	0.2908	96.53
LFP8	0.5999	1.0328	0.4691	0.2906	97.33
$LiFePO_4$/C	0.6000	1.0329	0.4691	0.2907	-
$LiFePO_4$ Standard	0.6010	1.0330	0.4692	0.2914	-

Firstly, the influences of the reaction concentration on the $LiFePO_4$ product were investigated, when the hydrothermal temperature was 180 ℃ for 16 h duration. Three $LiFePO_4$ samples (LFP1, LFP2, LFP3) prepared at different concentration (0.25, 0.50, 1.00 mol · L^{-1}) were obtained and tested subsequently. As shown in Fig.1 and Table 1, all the diffraction peaks and the lattice parameters (calculated by the software of Jade 5.0 from the XRD patterns) of the three samples match well with the standard orthorhombic $LiFePO_4$ (JCPDF: 40-1499), indicating good crystallinity of the three samples. The sample LFP2 shows strongest peak intensity among the three samples, certifying that LFP2 has the best crystallinity. As shown in Table 1, the yields (calculated from the ratio of the actual output and the theoretical output) of the three samples (LFP1, LFP2, LFP3) are 96.32%, 97.14%, 97.31%, respectively. The results show that the novel hydrothermal method has the relatively high yield for preparing $LiFePO_4$.

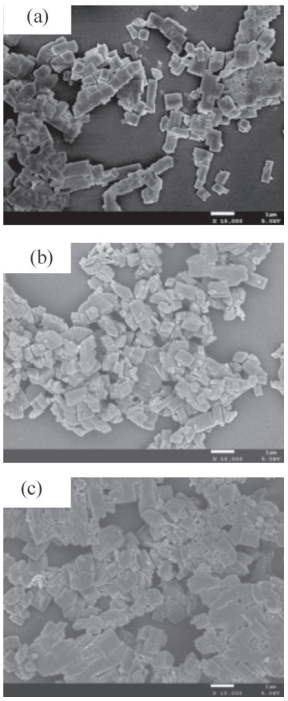

Fig.2 SEM images of the samples obtained with different concentrations at 180 ℃ for 16 h duration: (a) (LFP1) 0.25 mol · L^{-1}; (b) (LFP2) 0.50 mol · L^{-1}; (c) (LFP3)1.00 mol · L^{-1}

SEM images of the LFP1, LFP2 and LFP3 are presented in Fig.2. It is clear that three samples are mostly composed of small cubic particles. LFP1 synthesized at relatively low concentration (0.25 mol · L^{-1}) shows elongated morphology because of the oriented growth of crystal, and LFP3 shows obvious aggregation when the concentration is relatively high (1.00 mol · L^{-1}). LFP2 synthesized at 0.5mol L^{-1} concentration shows homogeneous shape and size, and the particle size is about 300 to 500 nm. Thus, the optimal concentration is 0.50 mol · L^{-1} in the experimental range of preparing $LiFePO_4$ via the novel hydrothermal method.

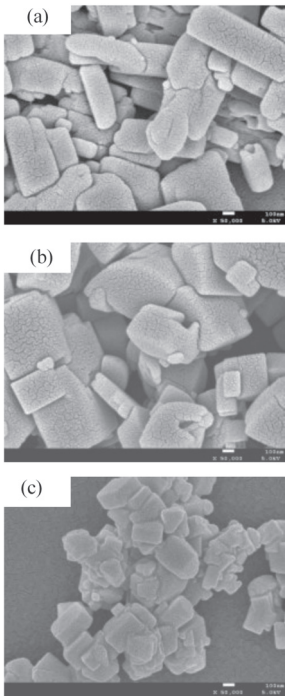

Fig.3 SEM images of the samples obtained with the fixed concentration of 0.50 mol · L^{-1} at different temperatures for 16 h duration: (a) (LFP4)140 ℃; (b) (LFP2) 180 ℃; (c) (LFP5) 200 ℃

The following three samples (LFP4, LFP2, LFP5) were prepared at the temperatures of 140, 180, and 200 ℃, respectively, with the fixed concentration of 0.5 mol · L^{-1} and reaction duration of 16 h. Fig.1 shows the XRD patterns of the three samples prepared at different hydrothermal temperatures. It is evident that all of the peaks in the three patterns and the lattice parameters (shown in Table 1) can be assigned to the standard $LiFePO_4$ pattern and the peak intensity increases slightly with the increase of the reaction temperature. The results suggest that the high hydrothermal temperature is beneficial for the improvement of the crystallinity of $LiFePO_4$ samples. SEM images of the three samples in Fig.3 show that the growth of the $LiFePO_4$ particles is imperfect at 140 ℃ and the particles show obvious aggregation at 200 ℃. It is evident that 180 ℃ is the optimal temperature to obtain fine morphology of $LiFePO_4$ particles. As shown in Table 1, the yields of the three samples (LFP4, LFP2, LFP5) are 96.58%, 97.14%, and 97.22% for $LiFePO_4$ synthesized at the temperatures of 140, 180, and 200 ℃, respectively, suggesting that high temperature is beneficial for increasing the yield of the $LiFePO_4$ product.

The first charge-discharge curves (at 0.1C between 2.5 and 4.3 V, 1C=170 mA · g^{-1}) of the three samples (LFP4, 140 ℃; LFP2, 180 ℃; LFP5, 200 ℃) are compared in Fig.4. The sample prepared at 180 ℃ has the largest capacity of 84.95 mAh · g^{-1} for the first cycle. The lower temperature and the higher temperature lead to the imperfect crystallization and particles aggregation, respectively, and result in poor electronic performance. In conclusion, the optimal reaction temperature to obtain high-quality $LiFePO_4$ electrode material is 180 ℃ in the experimental range of preparing $LiFePO_4$ via the novel hydrothermal method.

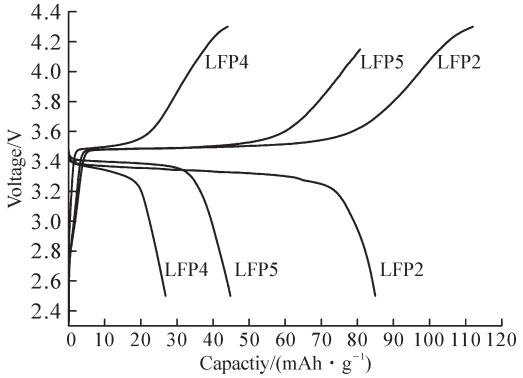

Fig.4 Charge-discharge curves (0.1C) of the three samples (LFP4, LFP2, LFP5) obtained at different hydrothermal temperatures (140 ℃, 180 ℃, 200 ℃)

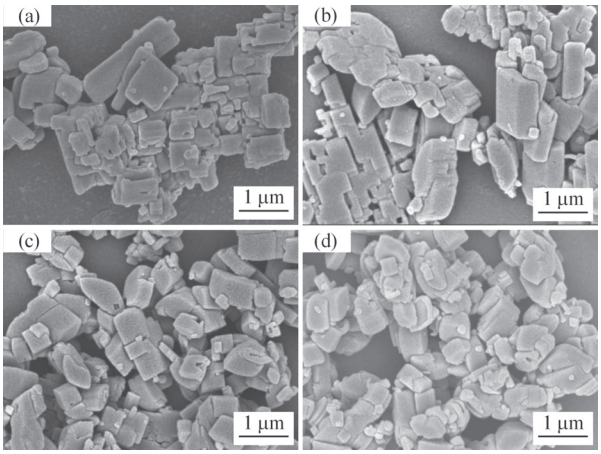

Fig.5 SEM images of the samples obtained at the fixed concentration of 0.50 mol · L^{-1} and temperature of 180°C for different durations: (a) (LFP6)4 h; (b) (LFP7) 8 h; (c) (LFP2)16 h; (d) (LFP8)20 h

The reaction duration usually affects the crystalline degree, particle size, morphology of resultant products. The following four samples (LEP6, LEP7, LEP2 and LEP8) were prepared at the duration of 4, 8, 16, and 20 h, respectively, with the fixed concentration of 0.5 mol · L^{-1} at the temperature of 180 ℃. Fig.1 shows the XRD patterns of the four samples. All of the four patterns and the lattice parameters (shown in Table 1) match well with standard orthorhombic $LiFePO_4$. The peak intensity increases slightly as the reaction duration increases from 4 h to 16 h, but there are no obvious differences between 16 h and 20 h.

SEM images of the four samples in Fig.5 show that the shorter duration (4 h and 8 h) and the longer duration (20 h) may lead to the imperfect growth and aggregation of the particles, respectively. It is evident that 16 h is the optimal duration to obtain fine morphology of $LiFePO_4$ particles. From Table 1, the yields of the four samples (LFP6, LFP7, LFP2, LFP8) are 96.11%, 96.53%, 97.14%, and 97.33% for $LiFePO_4$ synthesized at the duration of 4, 8, 16, and 20 h, respectively. As a result, the optimal reaction duration is 16 h in the experimental range of preparing $LiFePO_4$ via the novel hydrothermal method.

Table 2 The chemical compositions and the carbon content of the LFP2 and $LiFePO_4$/C samples

Sample	Li^+ /wt%	Fe^{2+}/wt%	Po_4^{3-}/wt%	C/wt%
LFP2	4.38	35.41	60.21	0
$LiFePO_4$/C	4.32	34.68	59.01	1.988

Based on the above investigations, the optimal conditions for preparing $LiFePO_4$ via the novel hydrothermal method are to set the reaction concentration at 0.5 mol · L^{-1}, the hydrothermal temperature at 180 ℃, and the hydrothermal duration at 16 h. The optimal sample (LFP2) with a pure phase, good olivine structure, homogeneous particle shape, small particle size (300 to 500 nm) and high yield is obtained. Moreover, the chemical compositions (analyzed by AAS) of the optimal sample (LFP2) are listed in Table 2. It can be concluded from Table 2 that the molar ratio of Li, Fe, P elements in $LiFePO_4$ is approximately 1:1:1, certifying that the optimal sample (LFP2) has the high purity.

3.2 Investigation of the mechanism of preparing $LiFePO_4$ by the novel hydrothermal method

The reports about the mechanism of applying the hydrothermal process to prepare $LiFePO_4$ are not too much. Lee J *et al*[26] reported that $Fe_3(PO_4)_2$•$8H_2O$ was the intermediate products, when LiOH, $FeSO_4$•$7H_2O$, and H_3PO_4 were applied as the starting materials (n(Li):n(Fe):n(P)=3:1:1). When the same starting materials and mixture ratio were used, $FeSO_4$ and H_3PO_4 should be mixed firstly and then LiOH was added, which could minimize the oxidation of $Fe(OH)_2$ to $Fe(OH)_3$, according to the opinion of Yang SF *et al*[27]. Padhi AK *et al*[28] believed that $FePO_4$ · $2H_2O$ could be generated when the lithium source was lacking. In this study, the relatively insoluble Li_2CO_3 is chosen as the lithium source to prepare $LiFePO_4$ via the novel hydrothermal method. As the novel hydrothermal process includes coating-precipitation reaction and hydrothermal conversion reaction, the mechanism of the novel hydrothermal course would be different from the traditional hydrothermal course of preparing $LiFePO_4$. In order to make clear the specific process and the mechanism of the novel hydrothermal course, the concentrations of Li^+ in the solution and the phase composition of the precipitates were detected at different reaction duration. The experiments were carried out by interrupting the reaction at different time, and the reaction concentration and temperature were fixed at 0.5 mol · L^{-1} and 180 ℃.

The reactions referred in the novel hydrothermal course are listed as follows:

$$HPO_4^{2-} \rightarrow H^+ + PO_4^{3-} \quad (1)$$

$$NH_4^+ + Fe^{2+} + PO_4^{3-} + H_2O \rightarrow NH_4FePO_4 \bullet H_2O\downarrow \quad (2)$$

$$Li_2CO_3 \leftrightharpoons 2Li^+ + CO_3^{2-} \quad (3)$$

$$Li^+ + NH_4FePO_4 \bullet H_2O \rightarrow LiFePO_4 + NH_4^+ + H_2O \quad (4)$$

The XRD patterns of the precursor resulted from the stage of coating-precipitation reaction show that the precursor is composed of Li_2CO_3 and NH_4FePO_4 · H_2O (Fig.6, 0 h). Therefore, in this stage, the reaction of $(NH_4)_2Fe(SO_4)_2$•$6H_2O$ with $(NH_4)_2HPO_4$ generates NH_4FePO_4•H_2O precipitate (reaction (1) and (2)), and the precipitate deposits on the surface of Li_2CO_3 particles, so that the process results in the formation of precursor with a core-shell structure. Fig.7 presents the TEM images of the coating-precipitation precursor and the elemental compositions on the surface of the core-shell precursor analyzed by EDS. The TEM images reveal that there is an obvious phase interface between the core and the shell and the EDS result reveals Fe and P elements existed on the surface of the precursor. Combined with XRD pattern of the precursor (Fig.6, 0 h) and related literature[29], we could conclude that

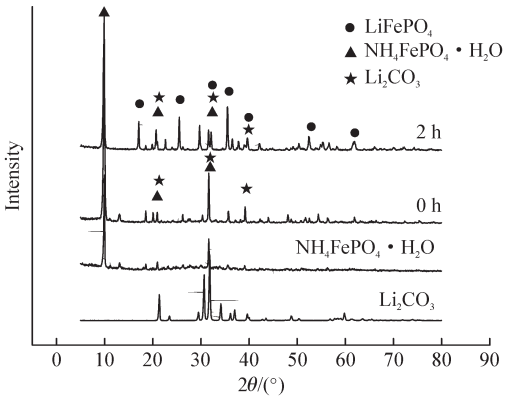

Fig.6 XRD patterns of the coating-precipitation precursor (0 h) and the product with hydrothermal conversion for 2 h comparing with Li_2CO_3 and NH_4FePO_4 · H_2O

the shell of the core-shell precursor is composed of NH_4FePO_4•H_2O (the gray parts in TEM images), and the core is composed of Li_2CO_3 (the black parts in TEM images).

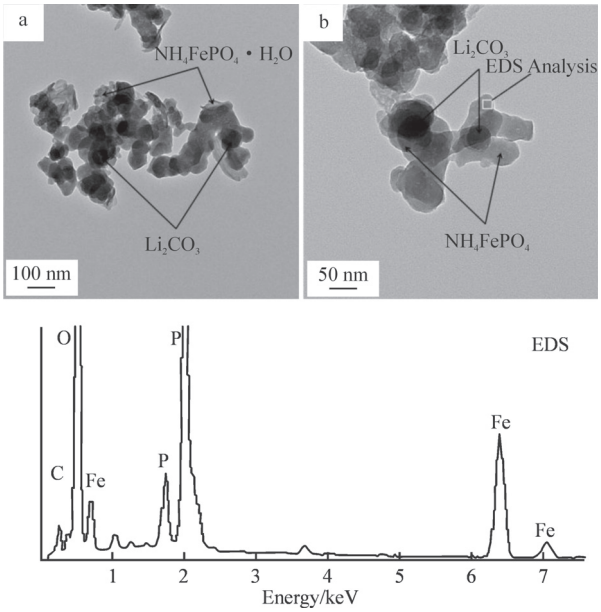

Fig.7 TEM images and EDS analysis of the core-shell coating-precipitation precursor

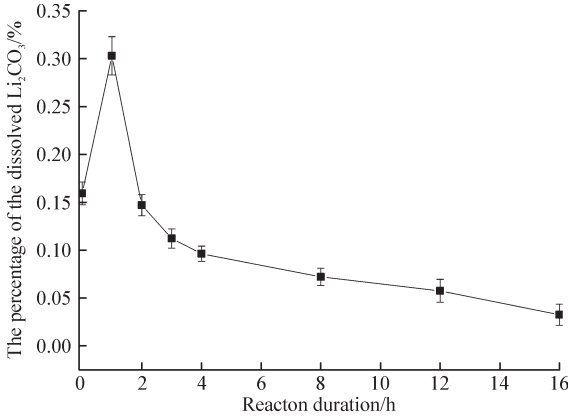

Fig.8 The concentration of Li_2CO_3 in the reaction solution, expressed as the molar percent of percent of initially solid Li_2CO_3

It could be also found from Fig.8 that the dissolved amount of Li_2CO_3 in the solution accounted for the percentage of initially used solid Li_2CO_3 is approximating 16% (calculated through the data obtained from AAS) in the precursor solution (when the reaction duration is 0 h). Regarding the possible reasons for the relatively high dissolved amount of Li_2CO_3, one is that Li_2CO_3 has certain solubility in water (the solubility is 0.71% at 100 ℃[30]), the other is that H^+ from the ionization of HPO_4^{2-} in $(NH_4)_2HPO_4$ (reaction (1)) can accelerate the dissolution of Li_2CO_3(reaction (3)).

In the stage of the hydrothermal conversion reaction, the dissolved amount of Li_2CO_3 in the hydrothermal solution increases remarkably during 0-1 h (Fig.8). When the reaction duration is 1h, the dissolved amount of Li_2CO_3 reaches to the maximum of 30.3% (Fig.9). There are two possible reasons: firstly, H^+ from the ionization of HPO_4^{2-} could further promote the dissolution of Li_2CO_3 because the NH_4FePO_4•H_2O on the surface of Li_2CO_3 is not compact; secondly, the hydrothermal system has not yet reached the steady state, which could result in the further dissolution of Li_2CO_3. During hydrothermal duration of 1-2 h, the concentration of the Li^+ in the hydrothermal solution has a clear downward trend, mainly because the dissolved Li^+ could displace NH_4^+ of NH_4FePO_4•H_2O to generate $LiFePO_4$ (Fig.6 certifies the formation of $LiFePO_4$ at 2 h); on the other hand, the hydrothermal system has reached the steady state, a part of the dissolved Li^+ could convert to Li_2CO_3 precipitation (the reverse of reaction (3)) because the solubility of Li_2CO_3 in the water decreases with increasing temperature[30]. After 2 h, the residual Li^+ in the solution consumes gradually through the reaction (4) to generate $LiFePO_4$. Meanwhile, the inside Li_2CO_3 in the core-shell structure could also react with neighboring NH_4FePO_4 • H_2O to generate $LiFePO_4$, the reaction process can still be explained as that the Li^+ dissolved from Li_2CO_3 displaces NH_4^+ of NH_4FePO_4•H_2O to generate $LiFePO_4$. When the reaction duration is 16 h, the concentration of Li^+ in the solution decreases to a relatively low level (Fig.8), indicating that most of the dissolved Li^+ converts to the $LiFePO_4$ product.

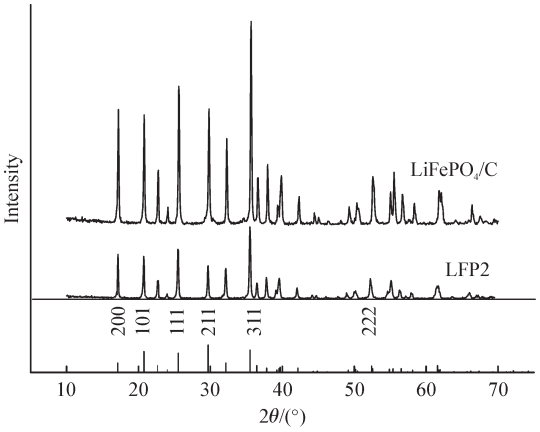

Fig.9 XRD patterns of LFP2 and $LiFePO_4$/C

3.3 Electrochemical performance of $LiFePO_4$/C

Although the optimal sample obtained from the hydrothermal process has the relatively high capacity of 84.95 mAh • g^{-1} for the first cycle, compared with

the theoretical capacity of $LiFePO_4$ (170 mAh · g^{-1}) the capacity is still not good. The lower capacity could be partly due to the imperfect crystallinity and the poor conductivity of the pure $LiFePO_4$ phase obtained by the hydrothermal course.

In order to overcome the above drawbacks, the optimal sample LFP2 mixed with glucose was calcined by two-step at 500 ℃ for 1h and 750 ℃ for 4 h under a N_2 (99.99%) flow to obtain the $LiFePO_4$/C composite. As shown in Fig.9, the $LiFePO_4$/C sample shows stronger peak intensity and narrower peak width, certifying the increase of crystallinity of the $LiFePO_4$ crystal. The added carbon in $LiFePO_4$/C has no corresponding diffraction peaks at detectable levels due to its low content or amorphous state. In addition, the chemical compositions (analyzed by AAS) and the carbon content (determined by EA) of $LiFePO_4$/C are listed in Table 2. It can be concluded from Table 2 that the carbon content in the $LiFePO_4$/C composite is 1.988% and the molar ratio of Li, Fe, P elements is approximately 1: 1: 1, certifying that the composite has relatively high purity.

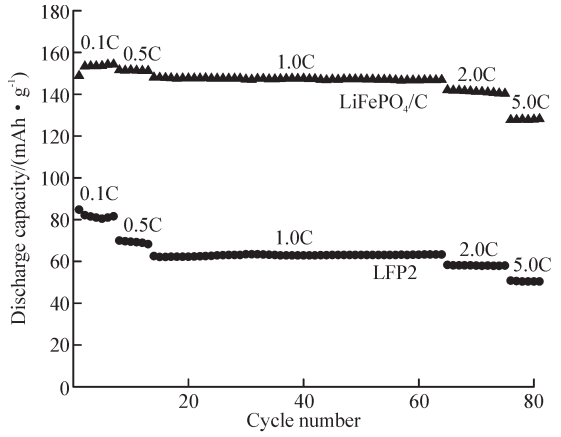

Fig.10 Rate capabilities of LFP2 and $LiFePO_4$/C

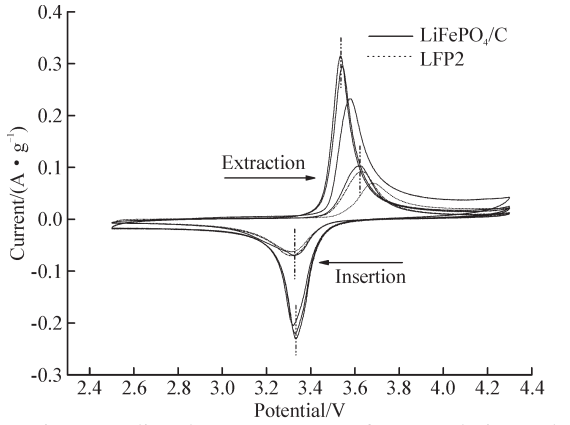

Fig.11 Cyclic voltammetry curves of LFP2 and $LiFePO_4$/C

Fig.10 shows the rate capabilities (at 0.1C and 5C rate) of LFP2 and $LiFePO_4$/C. The $LiFePO_4$/C composite exhibits better rate capacities compared with LFP2, and it also shows a high discharge capacity of 154.3 mAh · g^{-1} at 0.1C and 128.2 mAh · g^{-1} at 5C. The observation demonstrates that thermal treatment for the $LiFePO_4$ is necessary and an appropriate level of carbon has a good effect on the rate capacity of battery. Fig.11 shows the cyclic voltammetry curves of LFP2 and $LiFePO_4$/C composite. The $LiFePO_4$/C composite shows higher and sharper current peaks and smaller charge and discharge plateaus difference comparing with the sample of LFP2, implying better electrode reaction kinetics and better rate performance. The above results demonstrate that both the crystallinity and the conductivity of the $LiFePO_4$ material play a critical role in controlling the electrochemical performance of Li-ion batteries.

4 Conclusions

A novel hydrothermal method is proposed to prepare low-cost and high-performance $LiFePO_4$, in which Li_2CO_3 is chosen instead of traditional soluble lithium source to avoid the waste of lithium salt. The influences of the preparing conditions on the resultant $LiFePO_4$ samples were systematically investigated. As a result, the optimal conditions are to set the reaction concentration at 0.5 mol · L^{-1}, the hydrothermal temperature at 180 ℃, and the hydrothermal duration at 16 h. During the reaction course, the generated NH_4FePO_4•H_2O deposits on the surface of Li_2CO_3 substrates, resulting in the formation of precursor with a core-shell structure; then Li^+ dissolved from Li_2CO_3 gradually displaces NH_4^+ of NH_4FePO_4•H_2O to generate $LiFePO_4$. The optimized resultant $LiFePO_4$ with the well olivine crystal structure and small particle size of 300 to 500 nm exhibits a relatively high discharge capacity of 84.95 mAh · g^{-1} at the first charge-discharge cycle (0.1C). Moreover, the $LiFePO_4$/C composite obtained from two-step calcinations (500 ℃ and 750 ℃) of the mixture of the optimal $LiFePO_4$ sample and glucose under high-purity N_2 shows a high discharge capacity of 154.3 mAh · g^{-1} at 0.1C and 128.2 mAh · g^{-1} even at 5C; besides it has good reversibility and stability in CV test.

References

[1] Padhi AK, Nanjundaswamy KS, Goodenough JB. Phospho-Olivines as Positive-Electrode Materials for Rechargeable Lithium Batteries[J]. *J. Electrochem. Soc*., 1997, 144: 1 188-1 194

[2] Meligrana G, Gerbald C, Tue A, *et al*. Hydrothermal Synthesis of High

Surface $LiFePO_4$ Powders as Cathodes for Li-ion Cells[J]. *J. Power Sources*, 2006, 160: 516-522

[3] Shu HB, Wang XY, Wu Q, *et al.* The Effect of Ammonia Concentration on the Morphology and Electrochemical Properties of LiFePO4 Synthesized by Ammonia Assisted Hydrothermal Route[J]. *Eletrochim. Acta*, 2012, 76, 120-129

[4] Shenouda AY, Liu HK. Studies on Electrochemical Behaviour of Zinc-Doped $LiFePO_4$ for Lithium Battery Positive Electrode[J]. *J. Alloys Compd*., 2009, 477: 498-503

[5] Lee J, Teja AS. Synthesis of $LiFePO_4$ Micro and Nanoparticles in Supercritical Water[J]. *Mater. Lett*., 2006, 60: 2 105-2 109

[6] Vujković M, Stojković I, Cvjetićanin N, *et al*. Gel-Combustion Synthesis of $LiFePO_4$/C Composite with Improved Capacity Retention in Aerated Aqueous Electrolyte Solution[J]. *Eletrochim. Acta*, 2013, 92: 248-256

[7] Jones JL, Huang JT, Meng YS. Intermittent X-ray Diffraction Study of Kinetics of Delithiation in Nano-Scale $LiFePO_4$[J]. *J. Power Sources*, 2009, 189: 702-705

[8] Yu F, Zhang JJ, Yang YF, *et al*. Preparation and Characterization of Porous Spherical $LiFePO_4$/C by Spray Drying and Carbothermal Method[J]. *J. Wuhan University of Technology-Mater. Sci. Ed*., 2007, 22: 853-855

[9] Murugan AV, Muraliganth T, Manthiram A. Comparison of Microwave Assisted Solvothermal and Hydrothermal Syntheses of $LiFePO_4$/C Nanocomposite Cathodes for Lithium Ion Batteries[J]. *J. Phys. Chem. C*, 2008, 112: 14 665-14 671

[10] Yang JM, Bai Y, Qing CB, *et al.* Electrochemical Performances of Co-Doped $LiFePO_4$/C Obtained by Hydrothermal Method[J]. *J. Alloys Compd*., 2011, 509: 9 010-9 104

[11] Liang GC, Wang L, Ou XQ, *et al.* Lithium Iron Phosphate with High-Rate Capability Synthesized through Hydrothermal Reaction in Glucose Solution[J]. *J. Power Sources*, 2008, 184: 538-542

[12] Li XF, Zhang Z, Liu F, *et al*. Synthesis of Spherical $LiFePO_4$/C Composites as Cathode Material of Lithium-ion Batteries by a Novel Glucose Assisted Hydrothermal Method[J]. *Adv. Mater. Res*., 2013, 787: 58-64

[13] Li XF, Zhang X, Zhang Z. Synthesis of High-Performance $LiFePO_4$/C Composite with a Grape-Bunch Structure through the Hydrothermal Method [J]. *Ionics*, 2014, 20: 1 275-1 283

[14] Gao G, Liu AF, Hu ZH, *et al.* Synthesis of $LiFePO_4$/C as Cathode Material by a Novel Optimized Hydrothermal Method[J]. *Rare Metals*, 2011, 30: 433-438

[15] Brochu F, Guerfi A, Trottier J, *et al*. Structure and Electrochemistry of Scaling Nano C-$LiFePO_4$ Synthesized by Hydrothermal Route: Complexing agent effect[J]. *J. Power Source*, 2012, 214: 1-6

[16] Wang XF, Li T, Wu J, *et al*. Electrochemical Properties of Nano-LiFePO4 Prepared by Hydrothermal Reaction[J]. *J. Wuhan University of Technology-Mater. Sci. Ed*., 2011, 26(4): 624-627

[17] Kuwahara A, Suzuki S, Miyayama M, *et al.* Hydrothermal Synthesis of LiFePO4 with Small Particle Size and Its Electrochemical Properties[J]. *J. Electroceram*., 2010, 24, 69-75

[18] Chen J, Whittingham MS. Hydrothermal Synthesis of Lithium Iron Phosphate[J]. *Electrochem. Commun*., 2006, 8: 855-858

[19] Recham N, Armand M, Laffont L, *et al*. Eco-Efficient Synthesis of $LiFePO_4$ with Different Morphologies for Li-ion Batteries[J]. *Electrochem. Solid-State Lett.*, 2009, 12: A39-A44

[20] Doeff MM, Hu YQ, Mclarnn F, *et al*. Effect of Surface Carbon Structure on the Electrochemical Performance of $LiFePO_4$[J]. *Electrochem. Solid-State Lett.*, 2003, 6: A207-A209

[21] Yang ST, Zhao NH, Dong HY, *et al.* Synthesis and Characterization of $LiFePO_4$ Cathode Material Dispersed with Nano-Structured Carbon[J]. *Electrochim. Acta*., 2005, 51: 166-171

[22] Zhang Z, Peng SF, Liu DC. *Principle and Technology for Inorganic Fine Chemicals*[M]. Beijing: Chemical Industry Press, 2005:136-147

[23] Zhang Z, Li XF, Hu YL, *et al.* Chinese Patent, 2012, CN102790214A

[24] Kanamura K, Koizumi S, Dokko K. Hydrothermal Synthesis of $LiFePO_4$ as Cathode Material for Lithium Batteries[J]. *J. Mater. Sci.*, 2008, 43: 2 138-2 142

[25] Ou XQ, Xu SZ, Liang GC, *et al.* Effect of Fe(III) Impurity on the Electrochemical Performance of $LiFePO_4$ Prepared by Hydrothermal Process[J]. *Sci. China Ser. E*, 2009, 52: 264-268

[26] Lee J, Teja AS. Characteristics of Lithium Iron Phosphate ($LiFePO_4$) Particles Synthesized in Subcritical and Supercritical Water[J]. *J. Supercrit. Fluids*, 2005, 35: 83-90

[27] Yang SF, Zavalij PY, Whittingham MS. Hydrothermal Synthesis of Lithium Iron Phosphate Cathodes[J]. *Electrochem. Commun*., 2001, 3: 505-508

[28] Padhi AK, Nanjundaswamy KS, Masquelier C, *et al*, Effect of Structure on the Fe^{3+}/Fe^{2+} Redox Couple in Iron Phosphates[J]. *J. Electrochem. Soc*., 1997, 144: 1 609-1 613

[29] Li G, Yang ZX, Yang WS. Effect of $FePO_4$ Coating on Electrochemical and Safety Performance of $LiCoO_2$ as Cathode Material for Li-ion Batteries[J]. *J. Power Sources*, 2008, 183: 741-748

[30] Le ZQ, Bo SM, Wang GJ. *Inorganic Fine Chemicals Manual*[M]. Beijing: Chemical Industry Press, 2004:140-141